



Influence of the conductor network composites on the electromechanical performance of ionic polymer conductor network composite actuators

Sheng Liu^{a,*}, Reza Montazami^{c,1}, Yang Liu^a, Vaibhav Jain^d, Minren Lin^b, Xin Zhou^a, James R. Heflin^e, Q.M. Zhang^{a,b}

^a Department of Electrical Engineering, The Pennsylvania State University, University Park, PA 16802, United States

^b Materials Research Institute, The Pennsylvania State University, University Park, PA 16802, United States

^c Department of Materials Science and Engineering, Virginia Tech, Blacksburg, VA 24061, United States

^d Macromolecular Science and Engineering, Virginia Tech, Blacksburg, VA 24061, United States

^e Department of Physics, Virginia Tech, Blacksburg, VA 24061, United States

ARTICLE INFO

Article history:

Received 16 April 2009

Received in revised form 6 November 2009

Accepted 24 November 2009

Available online 29 November 2009

Keywords:

Electro-active polymers (EAPs)

Ionic actuators

Speed

Efficiency

Self-assembly

Layer-by-layer

ABSTRACT

We investigate the influence of conductor network composites (CNCs) on the electromechanical performance of the ionic polymer conductor network composite (IPCNC) actuators fabricated by the direct assembly method with ionic liquids as the solvent. It was observed that the newly developed IPCNCs with the layer-by-layer (LbL) self-assembled Au nanocomposite CNC layers exhibit a high strain response (~14% peak-to-peak strain) in comparison with that of IPCNCs with the traditional RuO₂/Nafion nanocomposite CNC layers (~6% peak-to-peak strain) under a 4 V DC signal. It is also observed that it is the slow ion transport process in the CNC layers that limits the IPCNC actuation speed and a thick CNC layer will result in a long ion transport time, slow actuation speed, as well as low efficiency. Making use of the fact that the LbL self-assembled nanocomposite CNCs can be made into thin layers (sub-micron) with high quality and large strain response, an IPCNC actuator with 0.4 μm thick of LbL CNC layers on 25 μm thick Nafion film exhibits an actuation response ~0.2 s with large bending actuation.

© 2009 Elsevier B.V. All rights reserved.

1. Introduction

In ionic conductive polymers, the accumulation or depletion of excess charges at the electrodes under an applied voltage will generate strain in these regions. This can be utilized for electromechanical transduction devices such as actuators and sensors [1–14]. Early work on Pt-electroded Nafion revealed a relatively large bending actuation in this ionic polymer metal composite (IPMC) under application of a few volts, which attracted a great deal of attention [4–6]. Since then, many research efforts have been devoted to this class of electroactive polymers (EAPs) with the objective of further improving the electromechanical performance such as the actuation speed, strain level, efficiency, and actuation lifetime [5–14].

Fig. 1(a) illustrates schematically such an ionic polymer bending actuator in which the accumulation and depletion of cations at the cathode and anode, respectively, create bending of the ionic polymer membrane under an electrical signal. Experiment-

tal results also indicated that a high population of the excess charges at the electrodes is highly desirable in order to generate high electromechanical actuation [5,12–13]. To realize that, porous electrodes which offer large electrode areas in contact with ionic polymers are often utilized in these actuators [4–14]. One of the widely investigated IPMCs uses a chemical reduction method to deposit precious metals on Nafion membrane surfaces, a perfluoro-sulfonated ionomer membrane developed by DuPont, in which nanosized metal particles penetrate into the Nafion membrane to form porous electrodes [4–7,12]. More recently, Akle and Leo developed a direct assembly method to fabricate porous electrode composites in which conductor nano-particles were mixed with a solution of an ionomer such as Nafion and this mixture is directly deposited on the Nafion (or other ionomer) membrane, which serves as the substrate [8,9,11,14]. The direct assembly method to fabricate IPMCs is attractive because it allows the use of a broad range of nanosized conductors for the electrodes including carbon nanotubes [11]. It also significantly simplifies the fabrication process of IPMCs, improves actuator performance, and enhances actuator manufacturing repeatability [11,14]. Illustrated in Fig. 1(b) is a typical bending actuator thus developed, which in general has a three layered structure, i.e., two porous composite electrode layers (conductor network composites (CNC)) separated by a neat

* Corresponding author.

E-mail address: szl139@psu.edu (S. Liu).

¹ These authors contributed equally to this work.

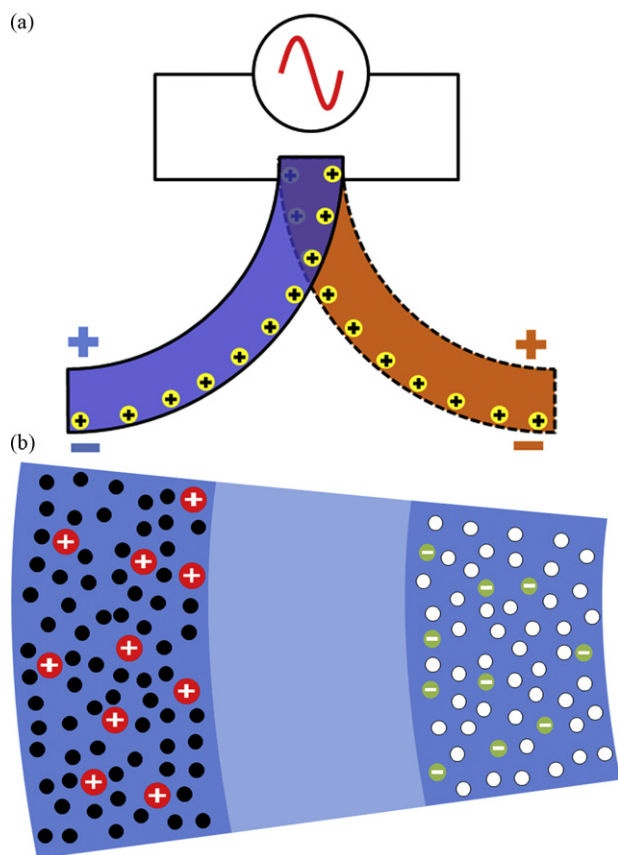


Fig. 1. (a) Schematic of an IPCNC bending actuator under an electric signal; (b) schematic of a composite/ionomer/composite (C/I/C) system (the external metal electrodes are not shown).

ionic polymer layer. To reflect the fact that the porous composite electrodes can be any type of interconnected electronic conductor networks, we refer to these composite electromechanical systems as an ionic polymer conductor network composite (IPCNC) in this paper.

IPCNC actuators are attractive because they can be operated under a few volts. On the other hand, IPCNC actuators generally suffer from low actuation speed which is often in the seconds or tens of seconds range and for many actuator applications, it is highly desirable to significantly improve the strain level, actuation speed, and efficiency [1,2,15]. In this paper, we investigate the influence of the CNCs on the electromechanical responses such as the strain level, actuation speed, and efficiency of IPCNCs fabricated by the direct assembly method. As will be shown in the paper, the actuator speed in these IPCNCs is closely related to the ion transport process in the CNC layer and a thin CNC layer will reduce the ion transport time, create fast actuation, and improve the electric efficiency. In this paper, a new class of CNC layer is investigated, which is based on layer-by-layer (LbL) self-assembled gold nano-particle composites [16–18]. This LbL CNC electrode can be made into submicron thin layers with high quality and reproducibility. As will be presented, an IPCNC actuator with LbL CNC layer thickness d_e of 0.4 μm and total actuator thickness of 25.8 μm displays an actuation response time ~ 0.18 s. Moreover, the high electromechanical strain generated in the LbL CNC layers (the peak to peak strain $\sim 14\%$) also causes a large bending actuation of the IPCNCs.

2. Experimental

Two classes of IPCNCs fabricated by the direct assembly method were examined in this paper. Besides the IPCNCs with the LbL CNCs,

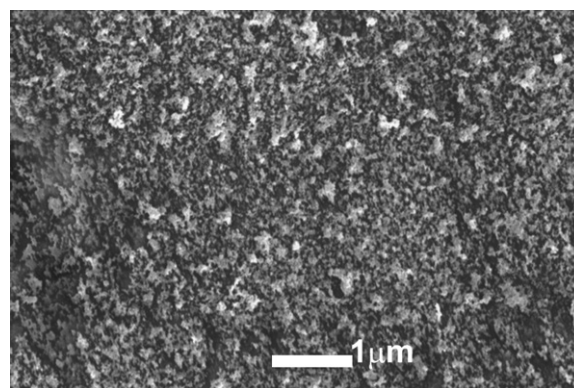


Fig. 2. SEM image of 100 bilayers LbL IPCNC surface.

IPCNCs with RuO_2 nanoparticle/Nafion composite CNCs, which have been studied extensively, were also investigated [8,9,14]. These two classes of IPCNCs allow the CNC layer thickness to be varied from sub-micron to more than tens of microns.

For the IPCNCs investigated in this paper, the commercial Nafion film NR-211 of thickness 25 μm was chosen as the ionomer layer in Fig. 1(b). LbL composites are made by immersing the Nafion film into two aqueous solutions alternately, which contain gold nanoparticles and poly(allylamine hydrochloride) (PAH) as the polyanion and polycation, respectively [18]. The composites grow via the electrostatic attraction between positively-charged PAH and the Nafion sulfonic groups or negatively-charged gold nanoparticles (particle size ~ 2 nm, Puresst Colloids, Inc.) [16–18]. The LbL CNCs, comprising 100 and 200 LbL bilayers, have the CNC electrode thickness d_e of 0.4 μm and 0.8 μm , respectively. For each IPCNC actuator, there are two CNC electrodes on two surfaces and hence the total IPCNC thickness is 25.8 and 26.6 μm , respectively. The IPCNCs with these two CNC layer thicknesses are referred to as LbL 1 and LbL 2 in the paper. An SEM image of a 100 bilayers LbL IPCNC surface is shown in Fig. 2. RuO_2 /Nafion composites are prepared using the direct assembly method [14]. RuO_2 nano-particles purchased from Alfa Aesar with 13–19 nm diameter are mixed with 20% Nafion dispersion from Aldrich. The mixture is sonicated before being sprayed on the Nafion film surface. In this study, a CNC layer with 40 vol% of RuO_2 nanoparticles was used [8,9,14]. After spraying, films are transferred to a vacuum oven to remove the solvent and then ready for further actuator fabrication.

After composites are grown on neat Nafion membranes, actuators are fabricated by soaking samples with 40 wt% ionic liquid 1-ethyl-3-methylimidazolium trifluoromethanesulfonate (EMI-Tf), which functions as the solvent as well as provides mobile ions for the actuation, and bonding 50 nm thick gold leaves as external electrodes on both sides of the samples [8,9]. As have been demonstrated, IPCNCs with ILs as the solvent to replace water can lead to many orders of magnitude increase in the actuation lifetime [8,9]. The lateral dimensions of all the actuators are 1 mm in width and 8 mm in length. Table 1 summarizes the thickness of the

Table 1
Summary of various thicknesses of the actuator films^a.

IPCNCs	Composite electrode thickness, d_e (μm)	Total thickness of the actuator (μm)
Neat Nafion 1	0	25
LbL 1	0.4	25.8
LbL 2	0.8	26.6
RuO_2 1	3	31
RuO_2 2	10	45
Neat Nafion 2	0	50

^a All actuators have lateral dimensions of 1 mm \times 8 mm (width \times length).

composite electrode layer d_e and the total thickness of the actuators investigated in this paper. For the comparison purpose, pure Nafion films with thickness of 25 and 50 μm which were bonded with 50 nm thick gold leaves on two sides of the film as the electrodes (Neat Nafion 1 and Neat Nafion 2 in Table 1), respectively, were also studied.

The time resolved bending actuation of the actuators was recorded by a charge coupled device (CCD) camera attached to a probe station (Cascade Microtech M150). A step voltage was applied to generate bending strain and the maximum applied voltage is 4 V. The actuation of these actuators as a function of frequency was also characterized under a 0.1 V AC signal. In the measurement, one end of the bending actuator is fixed and the tip displacement of the free end was measured by a laser vibrometer (OFV3001S controller and OFV 511 optical sensor head). The elastic modulus of each layer along the film surface direction in the IPCNC was characterized using a set-up specifically designed to measure the elastic modulus of soft materials [19–20]. In this set-up, the specimen is fixed at two ends and a displacement transducer was used to generate strain in the specimen and the corresponding stress (force/cross section area) was measured by a load cell. In this study, the elastic modulus of the Nafion film with 40 wt% EMI-Tf was measured first (≈ 50 MPa). Then the elastic modulus of the specimen with CNC layers deposited on the Nafion membrane was characterized. From this effective elastic modulus, the elastic modulus of the CNC layer can be deduced. For a bilayer laminate with the length much larger than the other dimensions as illustrated in Fig. 3, the measured elastic modulus Y^e is related to the elastic modulus of each layer Y^a

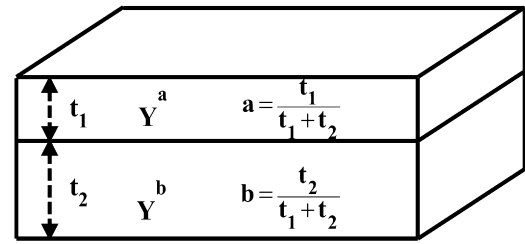


Fig. 3. Schematic of a bilayer laminate for the characterization of the elastic modulus of individual layers.

and Y^b as

$$Y^e = aY^a + bY^b \quad (1)$$

where a and b are the volume fractions of each layer in the laminate, respectively. The final effective elastic modulus of the five layered IPCNC absorbed with EMI-Tf was also measured from which the elastic modulus of the Au layer was deduced (≈ 20 GPa). The electrical impedance of these IPCNCs was characterized by a lock-in amplifier (Stanford Research System SR830 DSP) 0.1 V AC field amplitude. In this measurement, both the phase and amplitude of the applied voltage $V = V_0 \exp(j\phi_v)$ and current $I = I_0 \exp(j\phi_c)$ are recorded and the ratio yields the electric impedance Z as a function of frequency,

$$Z = \frac{V}{I} \quad (2)$$

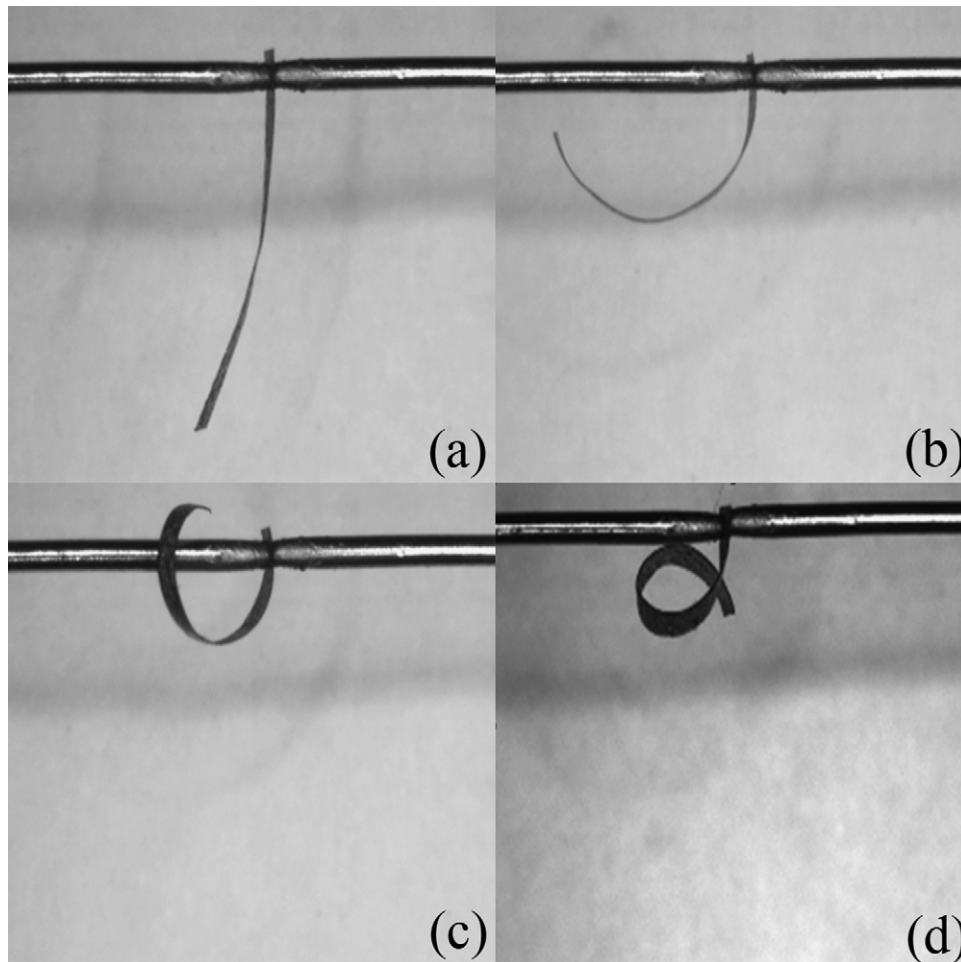


Fig. 4. Photo images of the bending actuation under 4V: (a) the neat Nafion layer of 25 μm thick; (b) the Lbl 1 (with 100 layers Lbl composite, 0.4 μm thick of each CNC layer) actuator; (c) the Lbl 2 (200 layers Lbl composite, 0.8 μm thick of each CNC layer) actuator; (d) the RuO₂ 1 (3 μm thick RuO₂/Nafion nanocomposite) bending actuator.

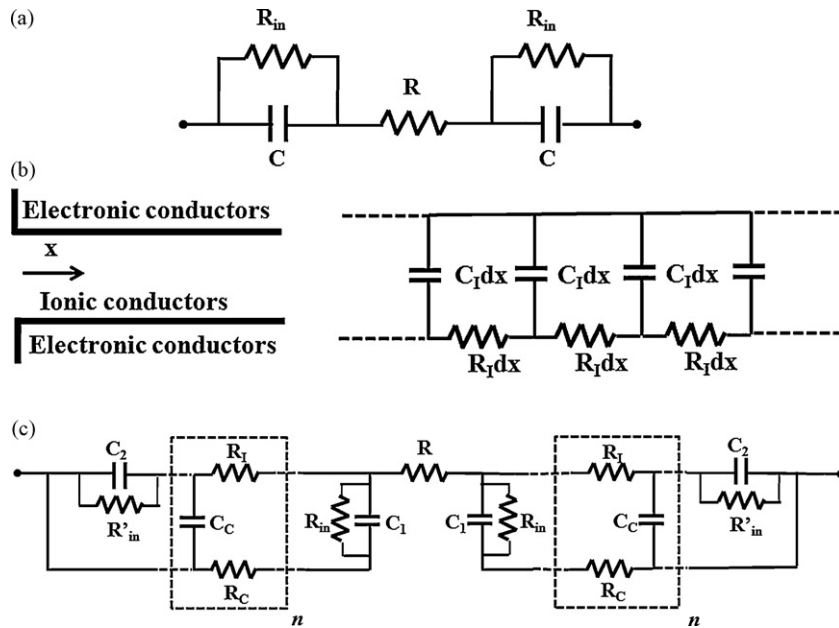


Fig. 5. (a) Equivalent electrical circuit for the pure ionomer with blocking electrodes; (b) RC transmission line for an ideal CNC with uniform pore along the thickness direction and high electronic conductance electrodes; (c) modified RC transmission line for an IPCNC actuator which consists of two CNCs separated by a Nafion layer. For the IPCNCs investigated here, the electronic resistance of the conductor networks cannot be ignored and is taken into consideration as R_e . For the completeness, the interphase EDL capacitors between the ionomers and electronic conductors are also included along with the resistors in parallel with them to take into account of leakage current at these interphases. n is the number of the RC units in the equivalent circuit of RC transmission line.

3. Results and discussion

3.1. Strain responses under high DC voltage (~4V)

Presented in Fig. 4(a) is the bending actuation of the actuators without the composite electrode layer, i.e. neat Nafion film of 25 μm thick with 40 wt% of ionic liquid EMI-Tf. The actuation is under a step voltage of 4V. The bending actuation is quite small due to the low electric double layer (EDL) capacitance from the flat electrodes of the neat ionomer films. Ionomeric polymer films such as Nafion with blocking electrodes form an electric double layer capacitor near the electrodes, due to the ion accumulation or depletion near the electrodes, and have been modeled as an interface EDL capacitor C at the electrodes in series with a resistor R which accounts for the conduction in the bulk of the film, as illustrated in Fig. 5(a) [21–23]. The resistance is given by $R=L/(A\sigma)$ where L is the Nafion film thickness, A is the area, and σ is the conductivity which is a product of mobile ion density n and mobility μ ($=qn\mu$, where q is the charge carried by the mobile ion). To take into account the leakage current at the electrode, a resistor R_{in} ($\gg R$) is often added in parallel with the EDL capacitor C [24]. The excess charges accumulated in the EDL capacitor C generate local strain near the electrodes and, for the case investigated here, create bending actuation when the strains at the cathode and anode are not the same [9].

As the CNC layer is added to the pure Nafion layer, the bending actuation increases markedly. As shown in Fig. 4(b), LbL 1 exhibits a much larger bending actuation even with only 0.4 μm thick LbL CNC layer on both sides of the 25 μm Nafion substrate. In general, for such a bending actuator under near static condition, a thicker CNC layer will generate larger bending and higher force output for a given CNC material.

In these actuators, the bending actuation is generated by the strains in the CNC layers. For bimorph bending actuators with a three layer structure, i.e., two active layers separated by an inactive layer, the relationship between the initial strain in the active layer and the bending radius of curvature R has been derived in the literature [25,26]. In order to extract the initial strain in the

CNC layer for the five-layer structure in Fig. 1(b), the relationship between the bending radius of curvature R and the initial strain S_0 along the film surface in the CNC layers (see Fig. 6) is derived here [25,26]. In the bending actuators, the actual strain S_1^c in the CNC layers is reduced due to the stresses from the ionomer layer and Au layer, i.e.,

$$S_1^c = S_{10}^c + s_{11}^c T_1^c \tag{3}$$

where s_{11}^c is the elastic compliance and T_1^c is the stress along the film surface.

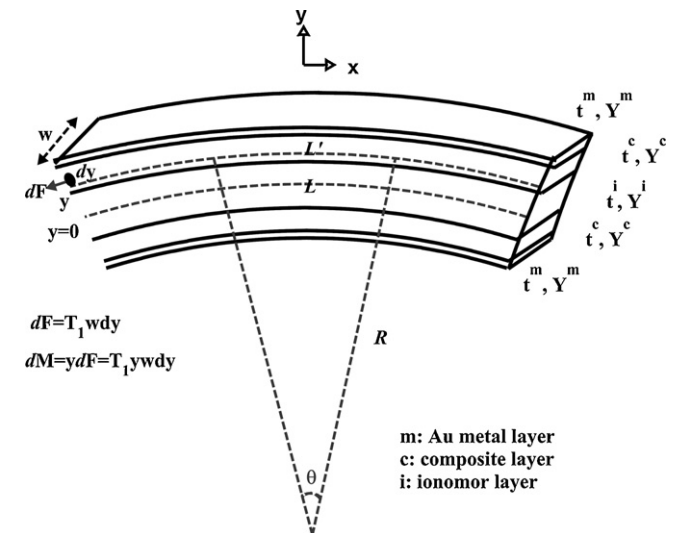


Fig. 6. A schematic for the five layer (Au/CNC/Ionomer/CNC/Au) bending actuator in Fig. 1b for the derivation of relation between the bending radius of curvature R and initial strain S_0 in the CNC layers.

For the bimorph actuator in Fig. 6, it can be derived that the strain S_1 is related to the radius of the curvature R .

$$S_1 = \frac{L' - L}{L} = \frac{(y + R)\theta - R\theta}{R\theta} = \frac{y}{R} = \kappa y \quad (4)$$

Substituting (4) into (3) and noticing that the elastic compliance s_{11}^c is the reciprocal of Young's Modulus Y^c , the stress T_1^c can be derived as

$$T_1^c = (s_{11}^c)^{-1} S_1^c - (s_{11}^c)^{-1} S_{10}^c = Y^c(\kappa y) \pm Y^c S_{10}^c \quad (5)$$

Similarly, for the ionomer and Au layers that do not generate initial strain S_0 , the stresses T_1^i and T_1^m can also be derived from their strains $S_1^i = s_{11}^i T_1^i$ and $S_1^m = s_{11}^m T_1^m$.

$$T_1^m = Y^m(\kappa y) \quad (6a)$$

$$T_1^i = Y^i(\kappa y) \quad (6b)$$

The superscripts c , i and m denotes the quantities in the composite, ionomer and Au metal layers, respectively. Since the actuator length is much larger than the thickness and width, we assume that all the other stress components are very small compared with T_1 so can be approximated as zero.

From the equilibrium conditions, when there is no external force or moment, the total moment M and total force F of the bending actuator satisfy $\int dF=0$ and $\int dM=0$. Assuming the strains in the two CNC layers of the bending actuator are the same in magnitude with opposite sign, the expanding force in upper half thickness is cancelled by the contracting force in the lower half thickness, and consequently $\int dF=0$ is true for any S_{10}^c value. Integrating over the thickness of $\int dM=0$, initial strain in the CNC layer S_{10}^c can be derived.

$$S_{10}^c = - \frac{Y^m \left(\frac{2t^m}{3} + 2t^m(t^c + \frac{t^i}{c}) \right)^2 + t^m(2t^c + t^i)}{RY^c(t^i t^c + t^c)} + Y^i \frac{t^i}{12} \quad (7)$$

From the radius of the curvature measured from several LbL 1 and LbL 2 bending actuators (Fig. 4), the strain S_{10}^c (amplitude) is derived to be $7 \pm 0.5\%$ under 4 V step voltage (or peak to peak strain $\sim 14\%$). In comparison, the strain S_{10}^c in the RuO₂ CNC layer deduced from the data is $3 \pm 0.5\%$ under the same voltage (or peak to peak strain $\sim 6\%$). The results obtained show that the LbL self-assembled Au nanocomposite CNC layers can generate much higher strain compared with RuO₂/Nafion nanocomposite based IPCNCs and other IPCNCs reported [13–15].

3.2. Frequency dependence and time response behaviors

The frequency dependence of the electromechanical strain and electrical impedance of these actuators as a function of frequency under 0.1 V AC signal was characterized to probe how the CNC layer thickness affects the frequency response of the actuator and the related electrical efficiency. It should be noted that the electrical and electromechanical responses of these ionic actuators are nonlinear functions of the applied voltage. Compared with high voltage responses, the linear electrical responses of these ionic conductive systems under low voltage have been relatively well understood [21–24]. In this study, we chose 0.1 V so that both the actuation strain and electric impedance can be characterized over a broad frequency range with required accuracy. We would like to point out that the applied voltage will affect the numerical values of the results, for example, the capacitance will increase with applied voltage in the voltage range studied here. However, these nonlinear effects will not change the conclusions drawn from the experimental results.

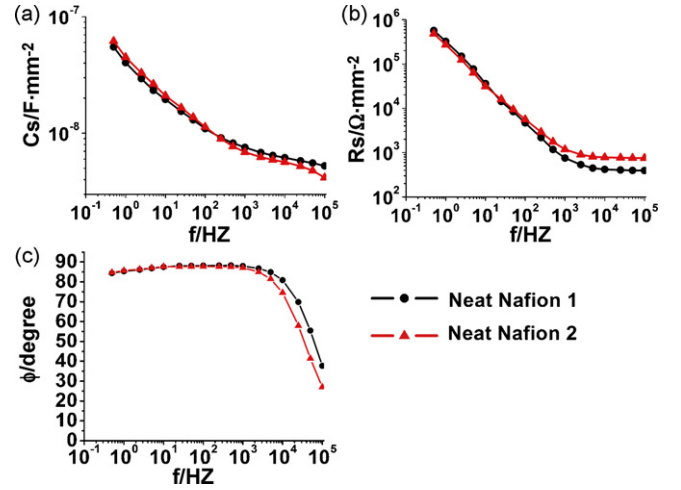


Fig. 7. Electrical impedance of neat Nafion films (Neat Nafion 1 of 25 μm thickness and Neat Nafion 2 of 50 μm thickness) as a function of frequency.

Fig. 7 present the electrical impedance of the neat Nafion layer, which can be understood based on the equivalent electrical circuit in Fig. 5(a) and for which the electrical impedance can be expressed as

$$Z = R_s + \frac{1}{j\omega C_s} \quad (8)$$

where $R_s = R + 2R_{in}/(1 + (\omega\tau_1)^2)$, $C_s = (1 + (\omega\tau_1)^2)C/2(\omega\tau_1)^2$, $\tau_1 = R_{in}C$, C is the electric double layer capacitance [21–24], R_{in} is related to the leakage current at the interface, and ω is the angular frequency. Under low applied voltage, it has been shown that C ($=\epsilon/L$, where L is the sample thickness and we assume the capacitor has a unit area) can be approximated as [21–23],

$$\epsilon = \epsilon_R \frac{1 + i\omega\tau}{i\omega\tau + \tanh(Y)/Y} \quad (9)$$

where ϵ_R is the dielectric permittivity of the material (i.e., Nafion with ILs here, $\epsilon_R = K\epsilon_0$, where K is dielectric constant), $\tau = \epsilon_R R/L = \epsilon_R/\sigma$, $\epsilon_0 = 8.85 \times 10^{-12}$ F/m (vacuum permittivity), $Y = M(1 + i\omega\tau)^{1/2}$, $M = L/(2L_D)$, and L_D is the Debye length which is in nm scale and much smaller than the film thickness. At low frequencies $C \sim \epsilon_R/L_D$ [21–23]. Hence, electrode polarization leads to significantly enhanced dielectric response. Eq. (8) can qualitatively describe the change of R_s and C_s with frequency in Fig. 7(a) and (b). Hence, when $\omega\tau_1 \ll 1$, C_s can be much larger than C while R_s is approaching $R + 2R_{in}$ and when $\omega\tau_1 \gg 1$ the electric impedance of Fig. 5(a) is $Z = R + 1/(j\omega C)$. For ionomers such as the Nafion films, it is well known that the EDL capacitor does not change while R will increase with film thickness [21–24]. Indeed, Fig. 7(a) and (b) shows that the capacitance of the neat Nafion films of 25 μm ($C \sim 6.2 \times 10^{-9}$ F mm^{-2}) is nearly the same as that of 50 μm thick ($C \sim 5.6 \times 10^{-9}$ F mm^{-2}), while R increases from 417 Ωmm^2 for the 25 μm thick film to 780 Ωmm^2 for the 50 μm thick film. The effective dielectric constant $K_{eff} = 15,890$ is deduced for 25 μm neat Nafion, in which $K_{eff} = \epsilon/\epsilon_0 = C/(L\epsilon_0)$. Such a large K_{eff} is due to the electrode polarization at the electrode interface [21–24]. The small variations in the R and C values are caused by the experimental uncertainties ($\pm 10\%$). All these values are taken at 10 kHz where both C_s and R_s become nearly independent of frequency and equal to C and R , respectively, because $\omega\tau_1 \gg 1$ at that frequency range. From the resistance value R , the conductivity of the Nafion film with IL of EMI-Tf at 10 kHz can be deduced as $\sigma = 6 \times 10^{-4}$ S cm^{-1} . In addition, by fitting Fig. 7(a) and 7(b) using Eq. (8) the values of R_{in} and τ_1 are obtained as $1 \times 10^4 \Omega \text{mm}^2$ and 7.2×10^{-3} s, respectively.

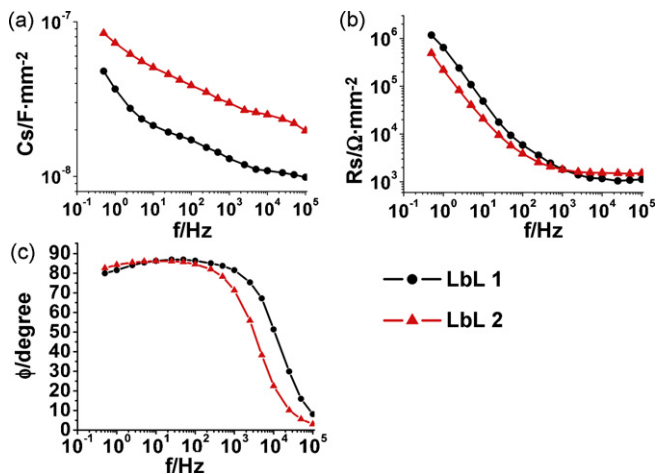


Fig. 8. Electrical impedance of LbL 1 and LbL 2 IPCNCs as a function of frequency.

Fig. 7(c) is the phase angle ϕ of the electrical impedance $Z = Z_0 \exp(j\phi)$ for the two Nafion layers as a function of frequency, where ϕ can be found from $\tan \phi = 1/\omega R_s C_s$. A $\phi = 90^\circ$ corresponds to a pure capacitor and $\phi = 0^\circ$ to a pure resistor (which would indicate the electrical impedance of the resistor is much larger than that of the capacitor which is $1/(\omega C)$). Since the resistive component represents the electrical loss, a ϕ approaches 90° is preferred in order to achieve a high electrical efficiency of the actuator. The data indicates that although these Nafion films exhibit small bending actuation due to low capacitance at the electrode, the small value of C_s and R_s results in a ϕ near 90° over a broad frequency range. To quantify this at high frequency end, we introduce the frequency f_1 at which $\tan \phi = 1$ (or $\phi = 45^\circ$) and the real (resistive) and imaginary (capacitive) parts of the electrical impedance become equal. For the neat Nafion films, the increased resistance from the films of 25–50 μm results in a reduction of f_1 from 79.3 to 43.7 kHz. The results indicate that for neat Nafion films, the electrical charge/discharge time can be quite short.

In general, the CNC porous electrode layer here is electrically very much similar to the porous electrodes used in the supercapacitors [24,27]. The ion transport in these porous electrodes, as shown by de Levie, is an electrical field driven diffusion process and for a uniform pore it can be modeled as a uniform RC transmission line as illustrated in Fig. 5(b) [24,27–32]. In the figure, C_1 is the unit length EDL capacitor formed at the electronic conductor and ionic conductor and R_1 is the unit length resistance of the ionic conductor. For the IPCNCs with complex porous electrodes such as the ones used here, the model needs to be modified as illustrated in Fig. 5(c), which is for the IPCNCs examined here and can still quantitatively explain the charge transport process in the CNC layers. In the figure, resistors R_c are added to take into account of the imperfect electrical contact among the conductive nanoparticles. However, in order for the CNCs to function as an effective porous electrode (low electronic resistance in the conductor network), $R_c \ll R_1$ where R_1 is the electrical resistance for the ion transport in the ionomers. For the simplicity, “dx” is removed in Fig. 5(c).

Fig. 8 presents the electrical impedance for the IPCNC actuators of LbL 1 and LbL 2 and Fig. 9 for RuO₂ 1 and RuO₂ 2. One noticeable change is that ϕ becomes smaller (less capacitive-like), especially for RuO₂ 2 which has 10 μm RuO₂/Nafion composite CNC layer, even at the lowest frequency measured (0.5 Hz), ϕ is at 55° . f_1 is also reduced significantly. For LbL 1 which is only 25.8 μm thick (0.4 μm CNC layer thickness on two sides of Nafion film), f_1 becomes 13.5 kHz. Further increasing the total CNC layer thickness to 0.8 μm reduces f_1 of LbL 2 actuator films to 3.64 kHz. For RuO₂ 1 and RuO₂ 2, which have total thickness of CNC electrode layers

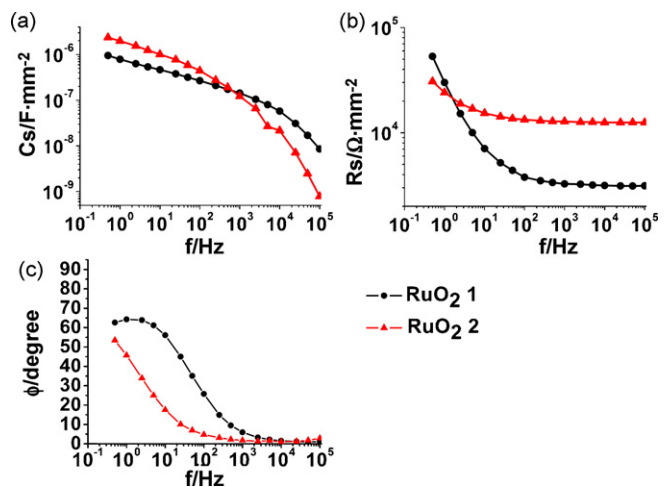


Fig. 9. Electrical impedance of IPCNCs with RuO₂/Nafion nanocomposite CNCs (RuO₂ 1 and RuO₂ 2) as a function of frequency.

of 3 and 10 μm , f_1 is reduced to 24.5 and 1 Hz, respectively. These results indicate that the charging time of IPCNC increases markedly as the CNC layer thickness increases and slow charging time in IPCNCs with thick CNC layers will limit the actuation speed (for most IPCNCs investigated, the CNC layer thickness is much larger than 10 μm).

For the IPCNC actuators with CNC electrodes, after the application of a voltage, excess ions will enter (or leave) the CNC porous electrode layer through the CNC/ionomer interface. Consequently, as indicated by the RC transmission line model in Fig. 5(c), the capacitors C_1 near the CNC/ionomer interface will be charged first and the excess ions will then progressively diffuse into the composite layer to charge the capacitors further away from the interface. Therefore, an IPCNC actuator with thicker CNC layer will have a longer ion transport time. Furthermore, due to the increased resistance in the charging (or discharging) process, as the frequency increases (or with short time electrical pulse), less capacitors in Fig. 5(c) will be charged for IPCNC with thick CNC layers. This explains the observed reduction (Fig. 9) of C_s for the RuO₂/Nafion based IPCNCs at frequencies above 1 kHz as the CNC layer thickness is increased from 3 to 10 μm .

The actuator electromechanical efficiency measures the percentage of energy conversion of the total input electrical energy to mechanical energy. Fig. 10 summarizes the pure electrical losses ($D = \tan(90 - \phi)$) of these IPCNC actuators and their comparison with the two neat Nafion films. The total input electrical energy into the actuator films includes the energy stored in the capacitors and resistive loss. It is the former that will be converted to mechanical energy for actuation and this conversion process has an efficiency η_{ME} which is below 100%. This is very similar to that in piezoelectric materials in which only a fraction of the electrical energy stored in the actuator capacitor component is converted into mechanical energy [33]. If there is no other loss, the total electromechanical conversion efficiency η_T which is the ratio of the mechanical energy generated to the total input electric energy is

$$\eta_T = \eta_e \times \eta_{ME} \quad (10)$$

where η_e is the ratio of the electric energy stored in the capacitor component to the total input electric energy ($=1/(1+D)$). For RuO₂ 2 which has a CNC layer thickness of 10 μm , η_e alone at 100 Hz is below 0.2 (20%).

In Fig. 11, we present the frequency dependence of the bending actuator tip displacement (\sim strain) of these actuators under 0.1 V AC signal as a function of frequency (Neat Nafion 1, LbL 1, and RuO₂ 1). At low frequencies, RuO₂ 1 displays larger tip displacement

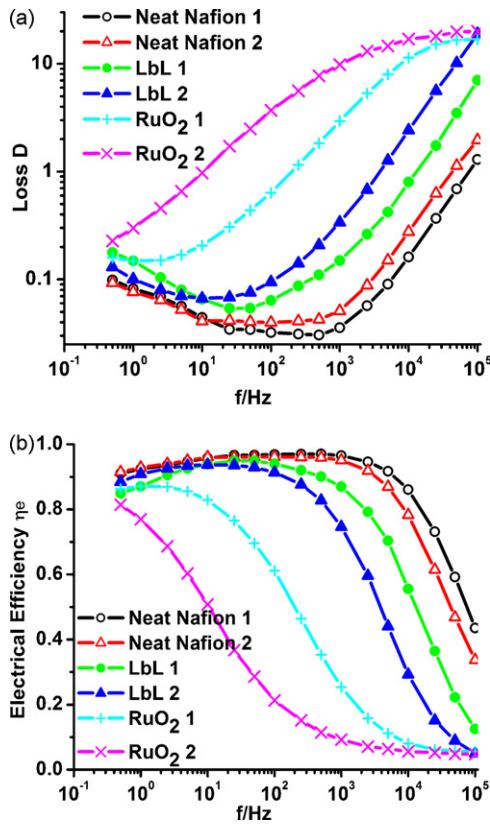


Fig. 10. (a) The electrical loss and (b) electrical efficiency of the IPCNCs.

ment due to the thick CNC layer (3 μm). However, at frequencies above 250 Hz, its tip displacement becomes smaller than that of LbL 1, caused by the fact that the penetration depth of the excess ions into the CNC layers in RuO₂ 1 becomes smaller (which also causes a reduction of the capacitance). In addition, an IPCNC actuator with thick CNC layers will require more excess ions in the CNC layer to generate the same bending compared with that with thin CNC layers.

From the data in Fig. 11, the strain S_{10}^c is calculated using Eq. (7) for LbL 1 and RuO₂ 1. Fig. 12 is the ratio of the strain S_{10}^c versus the charge stored in the CNC layer at the same frequency, which is

$$Q_0 = \frac{V_0 C_s}{\sqrt{1 + (\omega C_s R_s)^2}} \quad (11)$$

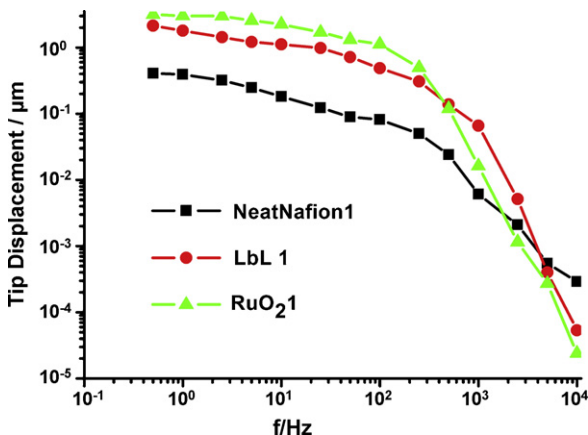


Fig. 11. Small signal (0.1 V amplitude AC) tip deflection as a function of frequency for Neat Nafion 1, LbL 1 and RuO₂ 1.

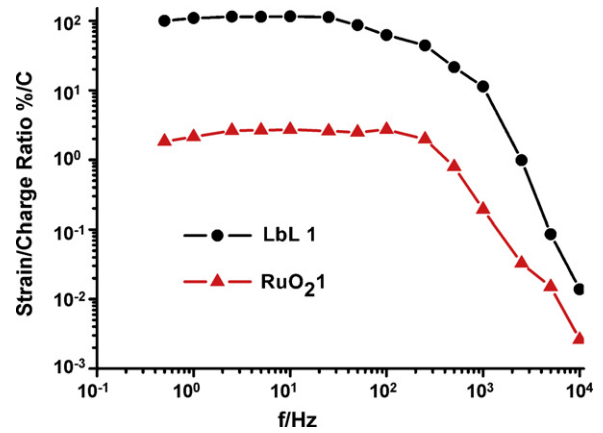


Fig. 12. The normalized ratio of strain to charge stored in the CNC layers as a function of frequency for LbL 1 and RuO₂ 1 (the data are divided by the maximum value in LbL 1 at 0.5 Hz).

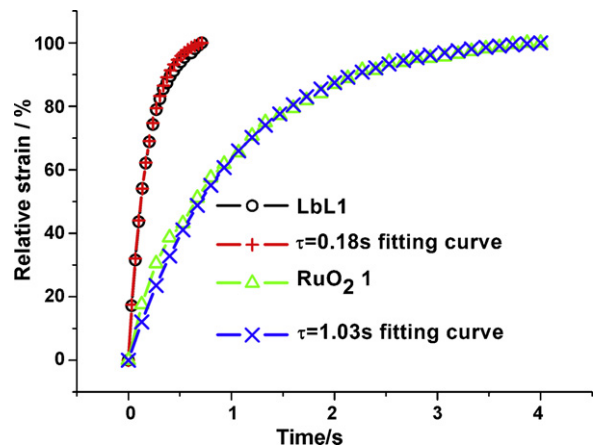


Fig. 13. The normalized time domain actuator strain (the data of each sample are divided by the maximum strain, respectively) under a step voltage of 4 V for LbL 1 and RuO₂ 1.

The results indicate that in the whole frequency range investigated (0.5–10 kHz) LbL 1 has much higher ratio of strain/charge compared with RuO₂ 1, implying much higher electromechanical conversion efficiency.

The bending actuation of LbL 1 and RuO₂ 1 under a step voltage of 4 V was characterized to probe the actuation speed. The thin CNC layers (~0.4 μm) lead to fast actuation response as presented in Fig. 13. Fitting the strain response in Fig. 13 with

$$S(t) = S_0(1 - e^{-t/\tau}) \quad (12)$$

where τ characterizes the actuation response time yields a τ = 0.18 s for the LbL 1 and τ = 1.03 s for RuO₂ 1 IPCNCs. A thin CNC layer can lead to fast IPCNC actuation response.

4. Conclusions

This paper investigates the influence of CNC layers on the electromechanical performance of IPCNCs fabricated by the direct assembly method. It shows that IPCNC actuators with CNC made of layer-by-layer self-assembled Au nanocomposite exhibit a high strain response (peak to peak strain ~14%) compared with that of IPCNC actuators with the traditional mixing method fabricated RuO₂ nanocomposite CNCs (peak to peak strain ~6%).

The LbL self-assembly process allows for fabricating high quality CNC layers with high reproducibility at submicron thickness which leads to fast actuation speed due to thin CNC layers. An IPCNC actu-

ator with 0.4 μm CNC layer exhibits a strain response time ~ 0.18 s under a step voltage of 4 V. The large strain in the CNC layers generates large bending actuation in these IPCNC actuators even with these thin CNC layers.

The frequency dependence behavior of these IPCNCs under low applied voltage (≈ 0.1 V) was also characterized at frequencies from 0.5 Hz to 10 kHz. The results show that LbL CNC based IPCNC actuators exhibit higher electrical efficiency and higher strain/charge ratio (higher electromechanical efficiency) compared with RuO₂/Nafion nanocomposite CNC based IPCNC actuators.

The results show the potential in developing CNCs for generating large strain response. The results also demonstrate that it is also the CNC layers in IPCNC actuators that determine the actuator speed. As the CNC layer thickness increases, the long ion transport time in the CNC layers results in a slow actuation response, which also causes a high electrical loss in the actuators.

In general, for an IPCNC actuator to deliver a large strain and force output, a large capacitance and hence a thick CNC layer is preferred. On the other hand, a thick CNC layer will lead to low actuation speed and low actuation response at high frequency. Hence, it is highly desirable to develop CNCs with very high electromechanical strain level and high ionic transport speed.

Acknowledgements

The authors thank Ralph Colby and Wenjuan Liu for many stimulating discussions regarding the works. This material is based upon work supported in part by the U.S. Army Research Office under Grant No. W911NF-07-1-0452 Ionic Liquids in Electro-Active Devices (ILEAD) MURI.

References

- [1] Y. Bar-Cohen (Ed.), *Electroactive Polymer (EAP) Actuators as Artificial Muscles*, SPIE EXPRESS, Bellingham, WA, 2004.
- [2] Y. Bar-Cohen, Q.M. Zhang, *Electroactive polymer actuators and sensors*, MRS Bull. 33 (2008) 173–181.
- [3] E.W.H. Jager, E. Smela, O. Inganas, *Microfabricating conjugated polymer actuators*, Science 290 (2000) 1540–1545.
- [4] K. Oguro, Y. Kawami, H. Takenaka, *Bending of an ion-conducting polymer film-electrode composite by and electric stimulus at low voltage*, J. Micromach. Soc. 5 (1992) 27–30.
- [5] K. Onishi, S. Sewa, K. Asaka, N. Fujiwara, K. Oguro, *Morphology of electrodes and bending response of the polymer electrolyte actuator*, Electrochim. Acta 46 (2000) 737–743.
- [6] M. Shahinpoor, *Microelectromechanics of ionic polymeric gels as electrically controllable artificial muscles*, J. Intell. Mater. Syst. Struct. 6 (1995) 307–314.
- [7] M. Shahinpoor, Y. Bar-Cohen, J.O. Simpson, J. Smith, *Ionic polymer–metal composites (IPMCs) as biomimetic sensors, actuators and artificial muscles – a review*, Smart Mater. Struct. 7 (1998) R15–R30.
- [8] B.J. Akle, M.D. Bennett, D.J. Leo, *High-strain ionomeric–ionic liquid electroactive actuators*, Sens. Actuators A 126 (2006) 173–181.
- [9] M.D. Bennett, D.J. Leo, *Ionic liquids as stable solvents for ionic polymer transducers*, Sens. Actuators A 115 (2004) 79–90.
- [10] I.S. Park, K. Jung, D. Kim, S.M. Kim, K.J. Kim, *Physical principles of ionic polymer–metal composites as electroactive actuators and sensors*, MRS Bull. 33 (2008) 190–195.
- [11] B.J. Akle, D.J. Leo, *Single-walled carbon nanotubes–ionic polymer electroactive hybrid transducers*, J. Intell. Mater. Syst. Struct. 19 (2008) 905–915.
- [12] S. Nemat-Nasser, Y.X. Wu, *Comparative experimental study of ionic polymer–metal composites with different backbone ionomers and in various cation forms*, J. Appl. Phys. 93 (2003) 5255–5267.
- [13] B.J. Akle, D.J. Leo, M.A. Hickner, J.E. McGrath, *Correlation of capacitance and actuation in ionomeric polymer transducers*, J. Mater. Sci. 40 (2005) 3715–3724.
- [14] B.J. Akle, M.D. Bennett, D.J. Leo, K.B. Wiles, J.E. McGrath, *Direct assembly process: a novel fabrication technique for large strain ionic polymer transducers*, J. Mater. Sci. 42 (2007) 7031–7041.
- [15] J.D.W. Madden, N.A. Vandesteeg, P.A. Anquetil, P.G.A. Madden, A. Takshi, R.Z. Pytel, S.R. Lafontaine, P.A. Wieringa, I.W. Hunter, *Artificial muscle technology: physical principles and naval prospects*, IEEE J. Ocean. Eng. 29 (2004) 706–728.
- [16] G. Decher, *Fuzzy nanoassemblies: toward layered polymeric multicomposites*, Science 277 (1997) 1232–1237.
- [17] P.T. Hammond, *Form and function in multilayer assembly: new applications at the nanoscale*, Adv. Mater. 16 (2004) 1271–1293.
- [18] V. Jain, H.M. Yochum, R. Montazami, J.R. Heflin, *Millisecond switching in solid state electrochromic polymer devices fabricated from ionic self-assembled multilayers*, Appl. Phys. Lett. 92 (2008) 033304.
- [19] K. Ren, Y.M. Liu, H. Hofmann, Q.M. Zhang, J. Blottman, *An active energy harvesting scheme with an electroactive polymer*, Appl. Phys. Lett. 91 (2007) 132910.
- [20] K.L. Ren, S. Liu, M.R. Lin, Y. Wang, Q.M. Zhang, *A compact electroactive polymer actuator suitable for refreshable Braille display*, Sens. Actuators A 143 (2008) 335–342.
- [21] R. Coelho, *On the static permittivity of dipolar and conductive media—an educational approach*, J. Non-Cryst. Solids 131 (1991) 1136–1139.
- [22] R.J. Klein, S.H. Zhang, S. Dou, B.H. Jones, R.H. Colby, J. Runt, *Modeling electrode polarization in dielectric spectroscopy: ion mobility and mobile ion concentration of single-ion polymer electrolytes*, J. Chem. Phys. 124 (2006) 144903.
- [23] J.R. Macdonald, *Theory of AC space-charge polarization effects in photoconductors, semiconductors, and electrolytes*, Phys. Rev. 92 (1953) 4–17.
- [24] B.E. Conway, *Electrochemical Supercapacitors*, Kluwer Academic/Plenum Publishers, New York, 1999.
- [25] J.M. Herbert, *Ferroelectric Transducers and Sensors*, Gordon and Breach, New York, 1982.
- [26] Q.M. Wang, L.E. Cross, *Performance analysis of piezoelectric cantilever bending actuators*, Ferroelectrics 215 (1998) 187–213.
- [27] J. Bisquert, A. Compte, *Theory of the electrochemical impedance of anomalous diffusion*, J. Electroanal. Chem. 499 (2001) 112–120.
- [28] R. de Levie, *On porous electrodes in electrolyte solutions *1. I. Capacitance effects*, Electrochim. Acta 8 (1963) 751–780.
- [29] A. Punning, U. Johanson, M. Anton, A. Aabloo, M. Kruusmaa, *A distributed model of ionomeric polymer metal composite*, J. Intell. Mater. Syst. Struct. 20 (2009) 1711–1724.
- [30] D. Pugal, K.J. Kim, A. Punning, H. Kasemagi, M. Kruusmaa, A. Aabloo, *A self-oscillating ionic polymer–metal composite bending actuator*, J. Appl. Phys. 103 (2008) 084908.
- [31] M. Porfiri, *Charge dynamics in ionic polymer metal composites*, J. Appl. Phys. 104 (2008) 104915.
- [32] M. Porfiri, *Influence of electrode surface roughness and steric effects on the nonlinear electromechanical behavior of ionic polymer metal composites*, Phys. Rev. E 79 (2009) 041503.
- [33] IEEE Standard on Piezoelectricity, ANSI/IEEE Std. 176–1987.

Biographies

Sheng Liu is currently pursuing his Ph.D. degree in the Department of Electrical Engineering of Pennsylvania State University, University Park. He received his B.S. degree in Physics from Nanjing University, Nanjing, China, in 2003 and M.S. degree in Electrical Engineering from Pennsylvania State University in 2008. His research interests include high performance electroactive polymers and composites devices, ion transport in ionic polymer and composites.

Reza Montazami received his B.S. in Physics from Virginia Tech and currently working on his Ph.D. in Materials Science and Engineering. His areas of interest are actuators and thin films.

Yang Liu received her B.S. degree in physics from University of Science and Technology of China, Hefei, China, in 2004 and received her M.S. degree in Physics from Northeastern University, Boston, MA in 2008. She is currently working toward the Ph.D. degree in the Department of Electrical Engineering, Pennsylvania State University, University Park. Her research interests include electroactive polymers & composites, solid state electromechanical devices such as actuator, supercapacitors and polymer related micro-electromechanical systems.

Vaibhav Jain received his Ph.D. at Virginia Tech in Macromolecular Science and Engineering in September 2009 and is currently working as a National Research Council Postdoctoral Researcher at Optical Sciences, Naval Research Laboratory, Washington, DC. His research work spans a range of topics in Polymer Science, Applied Physics and optoelectronics including the fabrication of fast-switching electrochromic devices for flat-panel displays, deposition of the nanoparticle stationary phase in MEMS-based columns for high-speed gas chromatography and fabricating bending and linear actuators for artificial muscles by ionic self-assembled multilayers (ISAMs). He has co-authored 10 publications and more than 20 conference presentations.

Minren Lin received his Ph.D. at University of Missouri, St. Louis in 1990 major in organometallics and catalysis. Then he had worked in the department of chemistry at the Pennsylvania State University in the field of catalytic system for methane conversion and polymerization as a research assistant and a senior research associate. He joined in Material Research Institute at the Pennsylvania State University in 2005, and has worked since then.

Xin Zhou received his Ph.D. degree in Electrical Engineering Department at the Pennsylvania State University. He received the B.S. degree in Electrical Engineering Department in Tsinghua University, China in 2002. His research focuses on electrical properties of polymeric materials, multilayers systems, and interfacial phenomena.

James R. Heflin is a professor of Physics at Virginia Tech, where he has been a faculty member since 1992. He received his Ph.D. in Physics from University of Pennsylvania in 1990. He is the Associate Director of the Center for Self-Assembled Nanostructures and Devices at Virginia Tech, an Associate Editor of the *International Journal*

of *Nanoscience*, and co-editor the textbook “Introduction to Nanoscale Science and Technology.” His research focuses on self-assembly of organic optoelectronic materials and devices.

Q.M. Zhang is a distinguished professor of electrical engineering and materials science and engineering of Pennsylvania State University. Dr. Zhang obtained Ph.D. in 1986 from Pennsylvania State University. The research areas in his group include fundamentals and applications of novel electronic and electroactive materials. Research activities in his group cover actuators and sensors, transducers, dielectrics and charge storage devices, polymer thin film devices, polymer MEMS, and electro-optic and photonic devices. He has over 270 publications and 10 patents (2 pending)

in these areas. His group has discovered and developed a ferroelectric relaxor polymer which possesses room temperature dielectric constant higher than 50, an electrostrictive strain higher than 7% with an elastic energy density $\sim 1 \text{ J/cm}^3$. His group also proposed and developed nano-polymer composites based on delocalized electron systems to raise the nano-polymeric composites dielectric constant near 1000. More recently, his group demonstrated a new class of polar-polymer with electric energy density over 25 J/cm^3 , fast discharge speed and low loss, attractive for high efficiency energy storage capacitors. He is the recipient of the 1999 Pennsylvania State Engineering Society Outstanding Research Award and a fellow of IEEE.